Structural and Functional Characteristics in Carriers of X-Linked Retinitis Pigmentosa with a Tapetal-Like Reflex

Mohamed A. Genead, MD, Gerald A. Fishman, MD, Martin Lindeman, COMT

Institute affiliation

Department of Ophthalmology and Visual Sciences, University of Illinois at Chicago, Chicago, Illinois, USA.

Correspondence to

Gerald A. Fishman, M.D.

Department of Ophthalmology and Visual Sciences (MC 648), Room 3.85, Eye and Ear Infirmary, 1855 W Taylor Street, Chicago, Illinois 60612-7234.

Tel: +1- 312-996-8939; Fax: +1-312-996-1950; email: gerafish@uic.edu

Address for requests of reprints

Department of Ophthalmology and Visual Sciences (MC 648), Room 3.85,

Eye and Ear Infirmary, 1855 W Taylor Street, Chicago, Illinois 60612-7234.

Tel: +1- 312-996-8939; Fax: +1-312-996-1950

Supported by funds from the Foundation Fighting Blindness, Owings Mills, Maryland; Grant Healthcare Foundation, Lake Forest, Illinois; NIH core grant EYO1792; and an unrestricted departmental grant from Research to Prevent Blindness.

The authors have no proprietary interests in this work.

Key Words: X-linked retinitis pigmentosa; tapetal-like reflex; microperimetry; fundus autofluorescence; and spectral-domain OCT.

Abstract

Purpose: to identify the functional and structural characteristics in three female obligate carriers of X-linked retinitis pigmentosa (XLRP) from the same family by using spectral-domain OCT (SD-OCT), fundus autofluorescence (FAF), and microperimetry (MP).

Methods: **Three female obligate carriers with a tapetal-like reflex (TLR), 21, 49, and 57 years of age, from a single family of XLRP that was seen in the ophthalmology department at the University of Illinois at Chicago, were enrolled in the study.** All carriers underwent a complete ophthalmic examination. SD-OCT measurements, a macular MP exam, and FAF testing were performed.

Results: The SD-OCT exam in all three carriers showed a normal retinal micro-structure and thickness. Microperimeter testing showed subnormal retinal sensitivity in the areas of the TLR. FAF exam showed the presence of speckled areas of enhanced AF.

Conclusions: Our study demonstrates that the carriers of XLRP with a TLR can show an enhanced reflectance on infrared images, abnormal autofluorescence properties, elevated retinal thresholds, and a normal retinal morphology within the posterior pole on SD-OCT testing

Introduction

Retinitis pigmentosa (RP) is the term applied to a clinically and genetically heterogeneous group of progressive retinal dystrophies. Patients develop progressive photoreceptor and retinal pigment epithelial (RPE) cell degeneration and, consequently, visual impairment. Initial visual symptoms include difficulty with night vision, peripheral vision and, ultimately, central vision.[1] X-linked RP (XLRP), presents with the early onset of clinically significant visual symptoms. It is the most severe genetic subtype of RP,[2,3] and accounts for 6-17% of familial RP cases.[3] While this genetic subtype produces a severe retinal degeneration in affected males, it shows an overall milder disease expression in female carriers.[4,5] Women who are carriers (heterozygotes) of XLRP usually have normal or close to normal visual acuity but often show some degree of fundus changes. These include a golden metallic-luster appearance within the perimacular area, referred to as a *tapetal-like reflex (TLR)*, and local areas of peripheral pigmentary changes.[4,6] A previous report by Grover et al.,[7] demonstrated that the degree of fundus change in carriers is important for their visual prognosis because carriers with only a tapetal-like reflex had a better prognosis for retinal visual function than those with peripheral pigmentation.

It has been accepted that the tapetal-like reflex (TLR) likely results from a random inactivation of one X-chromosome.[8] A previous study by Berendschot et al.,[9] showed an increased reflectance from the outer segments of the retinal photoreceptors in XLRP carriers with a TLR. Also, Cideciyan et al.,[10] showed that the TLR originated from cone photoreceptors and may result from the accumulation of a substance within cone inner segments.

Using linkage analysis, two major genetic loci were identified in XLRP, retinitis pigmentosa type 2 (*RP2*) and retinitis pigmentosa type 3 (*RP3*).[11-13] Mutations in *RPGR*, a retinitis pigmentosa GTPase regulator, are associated with the RP3 type of XLRP.[12] *RPGR* has been localized to the rod and cone photoreceptor connecting cilium,[14] which connects the outer with inner photoreceptor segments. Mutations within certain alleles of *RPGR* result in structural abnormality of the cilium.[15] It has been hypothesized that *RP2* may be involved in either cilium biogenesis or maintenance.[16]

The aim of our current study was to identify the functional and structural characteristics associated with the presence of a tapetal-like reflex in three female obligate carriers of XLRP from the same family by using spectral-domain OCT (SD-OCT), fundus autofluorescence (AF), and microperimetry (MP).

Materials and Methods

Subjects

Three female obligate carries of X-linked retinitis pigmentosa with a tapetal-like reflex from one family were enrolled in the study. The diagnosis was made based on the typical fundus appearance of a tapetal-like reflex within the posterior pole and significant family history of XLRP. Approval for the study was obtained from an Institutional Review Board at University of Illinois at Chicago and all the procedures followed the tenets of the Declaration of Helsinki. Informed consents was obtained from each of the participants.

Ocular Examination

All three female carriers underwent a complete ophthalmic examination that included determination of best-corrected visual acuity using ETDRS charts, slit-lamp biomicroscopic examination of the anterior segment, intraocular pressure measurements by Goldmann applanation tonometry, and dilated fundus examination by both direct and indirect ophthalmoscopy as well as biomicroscopy with a noncontact 78D lens. The three carriers, who were previously seen by one of the authors (G.A.F.), were contacted by telephone and asked to participate in the study based on their prior diagnosis of a carrier state for XLRP.

Ocular Imaging

SD-OCT was performed using a spectral-domain OCT/SLO system (Version 2.2, OPKO instrumentations/OTI, Miami, Florida, USA) to obtain both OCT and SLO images with an axial resolution of <10 microns, a transverse resolution of 20 microns (in tissue), and longitudinal and coronal (depth) scan range of 2.0 mm. The system used a confocal fundus image for alignment, orientation, and registration of the OCT image topographic maps for diagnostic purposes.

Both the Line scan (B-scan) and the 3D Retinal Topography scan protocols were used for image acquisition. The Line scan mode allows the capture of cross sectional B-scan OCT images of the vitreo-retinal, retinal, and chorio-retinal structures. A red scanning line on the SLO image represents the exact location of the cross sectional OCT image. We used the “Max Frame Count” of 32 frames. The “Max Frame Count” is the maximum sequentially captured frames of OCT and SLO images, which are captured and displayed

as individual frames. The 3D Retinal Topography mode covers an area of 9.0 x 9.0 mm with a 2.0 mm depth.

Fundus autofluorescence (FAF) was performed with a confocal laser scanning ophthalmoscope (cSLO) (Spectralis; Heidelberg Engineering, Heidelberg, Germany). Autofluorescence was excited by an argon blue wavelength (488 nm) and the emitted light above 500 nm was detected with the use of a barrier filter. Infrared (IR) reflectance images with a wavelength of 820 nm were obtained as well by the Spectralis system. Fundus color photography was also obtained on all three carriers. All the data obtained from the aforementioned testings were compared to three age-similar visually healthy subjects.

Macular Microperimetry (MP) Technique

MP was performed using the Spectral OCT/SLO system. All tests were performed after dilatation of the pupil with 1% tropicamide and 2.5% phenylephrine. Patching of the non-tested eye was performed. The carriers were instructed to fixate on a red square as a fixation target and press a bottom once they saw the stimulus light. A standard grid pattern (Polar 3 or 4), Goldmann III size stimulus, 200ms stimulus duration, and test strategy 4-2 parameters were used on all the carriers. The individual sensitivity values at 40 different loci within the central 12 degrees from each patient in our cohort were compared to normative data incorporated in the microperimeter software provided by the company for the Polar 3 test pattern within 95% and 99% confidence limits.

Results

The family pedigree is shown in **Figure 1**.

Case 1

A 49-year-old caucasian woman who was an obligate carrier had no ocular complaints. She came from a family with X-linked RP which had afflicted her father and two of her male cousins as well her sister's son. Vision was correctable to 0.20 LogMAR (20/30+1) OD and to 0.02 LogMAR (20/20-1) OS. The patient's manifest refraction was -7.25+2.00x125^{o} OD and -8.00+0.75x45^{o} OS. Ocular pressures were 18 mmHg OD and 16 mmHg OS. Color vision screening with Ishihara color plates was normal. The cornea, anterior chamber, and lenses were clear. The vitreous was fibrillar. Fundus exam showed a prominent choroidal pattern and changes consistent with high myopia. In addition, the patient had a tapetal-like reflex in each eye within the posterior pole. The optic discs and retinal vessels were normal. There were no peripheral retinal pigmentary degenerative changes in either eye **(Figure 2A, B)**.

A SD-OCT exam showed a normal retinal structure and thickness within the posterior pole. However, there was an enhanced reflectivity from the RPE-photoreceptor layer complex.

Fundus autofluorescence testing showed speckled areas of enhanced autofluorescence (AF) around the fovea and temporal to the macula which corresponded to the TLR **(Figure 2C)**.

Microperimetry testing of 40 individual points within a 6 degree radius from the center of the foveola (12 degree circle, Polar 3 pattern), showed subnormal individual point

thresholds within either a 95% or 99% confidence limit. Extension to an additional 4 degrees peripherally (16 degree circle, Polar 4 pattern) showed similar isolated points of reduced retinal sensitivity. The patient showed stable foveal fixation in each eye (100% of eye movements within 2 degrees around the projected fixation target OD and 99% OS) **(Figure 3)**.

Case 2

A 57-year-old caucasian woman (obligate carrier) had a son with X-linked RP. She did not have any visual complaints regarding her central, night, peripheral, or color vision. Vision was correctable to 0.06 LogMAR (20/20-3) OD with a -1.25 sphere and to 0.02 LogMAR (20/20-1) OS with a -1.00+0.50x60^{o}. Ocular pressures were 14 mmHg OD and 13 mmHg OS. Color vision screening with Ishihara color plates was normal. The cornea and anterior chamber were normal. Her lenses showed minimal nuclear sclerosis in each eye.

Fundus exam showed a tapetal-like reflex within the posterior pole in each eye. The optic disc and retinal vessels were normal. There were no peripheral retinal pigmentary degenerative changes in either eye.

SD-OCT exam showed normal retinal structure and thickness within the posterior pole. Fundus autofluorescence testing showed diffuse speckled and patchy areas of enhanced AF within the posterior segment of the retina. Also, the FAF image showed the presence of a parafoveal ring of AF. Infrared imaging showed an enhanced reflectivity within the area of the TLR **(Figure 4)**.

Microperimetry testing within a 6 degree radius from the center of the foveola (12 degree circle, Polar 3 pattern), showed subnormal isolated point thresholds within either a 95%

or 99% confidence limit. Extension to an additional 4 degrees peripherally (16 degree circle, Polar 4 pattern) showed similar isolated points of reduced retinal sensitivity. The patient showed relatively stable foveal fixation in the right eye (87% of eye movements within 2 degrees around the projected fixation target OD) and a stable foveal fixation in the left eye (99% of eye movements within 2 degrees around the projected fixation target OS) **(Figure 5)**.

Case 3

A 21-year-old caucasian girl (obligate carrier) had a brother with X-linked RP. The patient did not have any subjective ocular complaints. Vision was correctable to 0.12 LogMAR (20/25+1) OD with a -8.75+0.75x165^{o} and to 0.08 LogMAR (20/20-2) OS with a -9.25+0.25x125^{o}. Ocular pressures were 12 mmHg OD and 11 mmHg OS. Color vision screening with Ishihara color plates was normal. The anterior segment exam was unremarkable. Fundus exam showed an extensive tapetal-like reflex within the posterior pole more prominently temporal to the macula in each eye. The optic disc and retinal vessels were normal. There were no peripheral pigmentary degenerative changes in either eye.

SD-OCT exam showed a normal retinal structure and thickness within the posterior pole. Also there was an enhanced reflectivity from the RPE-photoreceptor layer complex **(Figure 6)**. Fundus autofluorescence testing showed similar findings to those observed in Case 2 with diffuse speckled and patchy areas of enhanced autofluorescence within the posterior segment of the retina.

Microperimetry testing within a 6 degree radius from the center of the foveola (12 degree circle, Polar 3 pattern) showed isolated patchy areas of subnormal thresholds within

either a 95% or 99% confidence limit. Extension to an additional 4 degrees peripherally (16 degree circle, Polar 4 pattern) showed similar isolated points of elevated retinal thresholds in this region. The patient showed stable foveal fixation in each eye (98% of eye movements within 2 degrees around the projected fixation target OD and 99% OS).

Discussion

The aim of the current study was to identify the functional and structural characteristics associated with a TLR in three female obligate carriers of XLRP from the same family by using spectral-domain OCT, fundus autofluorescence, and macular microperimetry.

The TLR is one of the two fundoscopically detectable abnormalities seen in carriers of XLRP, the other being peripheral pigmentary degenerative changes.[7] Cideciyan and coworkers showed that the TLR appeared to be made up of radiating sectors which were composed of small round unit reflexes from reflective particles in the cone inner segments.[10] This observation was consistent with the finding of intracellular lipid droplets in some types of tapeta in animals.[17]

Investigators have described the TLR as lying deep to the retinal blood vessels and at the level of the outer retina and RPE. However, previous fluorescein angiography studies showed no abnormalities in the areas of the TLR.[18] It has been suggested that the TLR could be the result of deposits, thickening, or degeneration in Bruch's membrane, deposits in the retina, or an alteration at the level of RPE-photoreceptor interface. The presence of a fundus reflex resembling the TLR in XLRP carriers has also been observed

in patients with cone dystrophy. This led to the suggestion that the TLR indicated involvement of the cone photoreceptors.[10]

Infrared reflectance (IR) images, which use an excitation wavelength of 820 nm, provide information about the deep retinal structures and the integrity of the RPE layer. IR has several advantages when compared with normal fundus photography and FAF modalities, including the ability to penetrate cloudy media such as cataracts. Our study showed that IR images disclosed an enhanced and more detailed image of the TLR in all three of our carriers.

The use of FAF imaging can visualize retinal abnormalities prior to fundoscopically visible changes or certain fundus changes can show corresponding defects on AF. We observed the presence of an abnormal AF pattern in our carriers in the form of diffuse areas of speckled and patchy enhanced AF. This observation was similar to a previous study by Wegscheider et al.,[19] who described different abnormal AF patterns in carriers of XLRP such as the presence of a clear radial pattern of locally increased AF or the presence of a more annular, slightly irregular pattern, with increased AF surrounding the fovea. Additionally, our finding on FAF is consistent with that of Reese et al.,[20,21] who described the occurrence of distinct patterns of radial (rod) and tangential (cone) dispersion during clonal expansion early in photoreceptor cell differentiation.

Our study cohort showed an extrafoveal ring of enhanced AF in some of the carriers (Cases 2 and 3). We hypothesize that the genetic defects in *RPGR* or *RP2* genes, which lead to dysfunction in the connecting cilium of the photoreceptor cells, could result in an accumulation of a retinoid compound(s) in the inner segments of the photoreceptors

which, in turn, could account for the enhanced AF. This hypothesis is consistent with the finding that certain retinoids may show weak autofluorescence.[22] Mohand and co workers[23] showed that the area of enhanced AF corresponded with the ring of high rod density that surrounds the fovea. Since rod outer segments are shed on an ongoing basis, enhancement of AF in this area could result from a higher turnover rate and therefore greater accumulation of lipofuscin within a zone of high rod density.[23]

On MP testing, a reduced retinal sensitivity within the areas with enhanced AF and the TLR was observed. This finding was similar to a previous report by Wegscheider et al.,[19] who detected matching sensitivity losses in areas with increased AF in carriers of XLRP. However, an observed elevated retinal threshold might be due to either the carrier state itself (the genetic abnormality) or to an associated highly myopic refractive error (observed in 2 of our 3 carriers).

Of interest, our three carriers showed what appeared to represent an increase in the RPE-photoreceptor layer complex reflectivity which is consistent with a previous study by Vingolo et al.,[24] that showed increased RPE reflectivity or changes in retinal thickness on OCT testing in carriers of XLRP.

In conclusion, our study of three XLRP carriers with a TLR demonstrated enhanced reflectance on infrared images, abnormal autofluorescence properties, and elevated retinal thresholds in the presence of normal retinal morphology within the posterior pole on SD-OCT testing.

References

1. Marmor MF, Aguirre G, Arden GB, et al. Retinitis pigmentosa: A symposium on terminology and methods of examination. Ophthalmology. 1983; 90:126-131.
2. Fishman GA. Retinitis pigmentosa. Genetic percentages. Arch Ophthalmol. 1978; 96:822-826.
3. Bird AC. X-linked retinitis pigmentosa. Br J Ophthalmol. 1975; 59:177-199.
4. Fishman GA, Weinberg AB, McMahon TT. X-linked recessive retinitis pigmentosa: clinical characteristics of carriers. Arch Ophthalmol. 1986; 104:1329-1335.
5. Brouzas D. Psychophysical tests in X-linked retinitis pigmentosa carrier status. Surv Ophthalmol. 1995; 39:76-84.
6. Falls HF, Cotterman CW. Choroidal degeneration: A sex-linked form in which heterozygous women exhibit a tapetal-like reflex. Arch Ophthalmol. 1948; 40:685-703.
7. Grover S, Fishman GA, Anderson RJ, Lindeman M. A longitudinal study of visual function in carriers of X-linked recessive retinitis pigmentosa. Ophthalmology. 2000; 107(2):386-396.
8. Krill AE. Observations of carriers of X-chromosomal-linked chorioretinal degenerations. Do these support the “inactivation hypothesis”? Am J Ophthalmol. 1967; 64:1029-1040.
9. Berendschot TT, DeLint PJ, van Norren D. Origin of tapetal-like reflexes in carriers of X-linked retinitis pigmentosa. Invest Ophthalmol Vis Sci. 1996; 37(13):2716-2723.

10. Cideciyan AV, Jacobson SG. Image analysis of the tapetal-like reflex in carriers of X-linked retinitis pigmentosa. Invest Ophthalmol Vis Sci. 1994; 35(11):3812-3824.

11. Teague PW, Aldred MA, Jay M, et al. Heterogeneity analysis in 40 X-linked retinitis pigmentosa families. Am J Hum Genet. 1994; 55(1):105-111.

12. Meindl A, Dry K, Herrmann K, et al. A gene (RPGR) with homology to the RCC1 guanine nucleotide exchange factor is mutated in X-linked retinitis pigmentosa (RP3). Nat Genet. 1996; 13(1):35-42.

13. Mears AJ, Gieser L, Yan D, et al. Protein-truncation mutations in the RP2 gene in a North American cohort of families with X-linked retinitis pigmentosa. Am J Hum Genet. 1999; 64(3):897-900.

14. Hong DH, Pawlyk BS, Shang J., et al. A retinitis pigmentosa GTPase regulator (RPGR)-deficient mouse model for X-linked retinitis pigmentosa (RP3). Proc Natl Acad Sci U S A. 2000; 97(7):3649-3654.

15. Rohlich P. The sensory cilium of retinal rods is analogous to the transitional zone of motile cilia. Cell Tissue Res. 1975; 161:421-430.

16. Hardcastle AJ, Thiselton DL, Van Maldergem L, et al. Mutations in the RP2 gene cause disease in 10% of families with familial X-linked retinitis pigmentosa assessed in this study. Am J Hum Genet. 1999; 64(4):1210-1215.

17. Bird AC, Marshall J. Retinal receptor disorders without known metabolic abnormalities. In: Garder A, Klintworth GK, eds. Pathobiology of Ocular Disease. New York: Marcel Dekkar; 1982:1167-1220.

18. Noble KG, Margolis S, Carr RE. The golden tapetal sheen reflex in retinal disease. Am J Ophthalmol. 1989; 107:211-217.

19. Wegscheider E, Preising MN, Lorenz B. Fundus autofluorescence in carriers of X-linked recessive retinitis pigmentosa associated with mutations in RPGR, and correlation with electrophysiological and psychophysical data. Graefes Arch Clin Exp Ophthalmol. 2004; 242(6):501-511.

20. Reese BE, Harvey AR, Tan SS. Radial and tangential dispersion patterns in the mouse retina are cell-class specific. Proc Natl Acad Sci U S A 1995;92:2494–2498

21. Reese BE, Necessary BD, Tam PP, Faulkner-Jones B, Tan SS. Clonal expansion and cell dispersion in the developing mouse retina. Eur J Neurosci 1999;11:2965–2978

22. Imanishi Y, Batten ML, Piston DW, Baehr W, Palczewski K. Noninvasive two-photon imaging reveals retinyl ester storage structures in the eye. J Cell Biol. 2004; 164(3):373-383.

23. Mohand-Said S, Hicks D, Leveillard T, Picaud S, Porto F, Sahel JA. Rod-cone interactions: developmental and clinical significance. Prog Retin Eye Res 2001; 20:451–467.

24. Vingolo EM, Livani ML, Domanico D, Mendonça RH, Rispoli E. Optical coherence tomography and electro-oculogram abnormalities in X-linked retinitis pigmentosa. Doc Ophthalmol. 2006; 113(1):5-10.

Figure Legends

Fig.1 The family pedigree of our cohort; case 1 is (III 2), case 2 (III 3), and case 3 (IV 4).

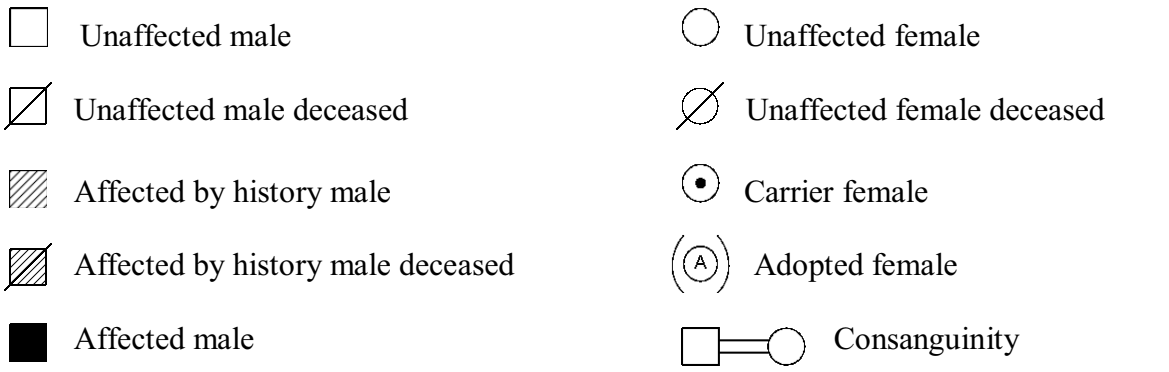

Fig. 2 Fundus photograph of the left eye of case 1 shows fundus TLR within the posterior pole more prominent temporal to the macula (A). Infrared (IR) image (B) demonstrates an enhanced reflectivity within the area of the TLR. Autofluorescence (AF) image (C) shows speckled regions of enhanced AF which correlated with the fundus TLR.

Fig.3 Microperimetry testing results from each eye of case 1 shows isolated patchy areas of subnormal retinal thresholds within the posterior pole. The right eye is on the right and left eye on the left.

Fig.4 Fundus photograph of the right eye of case 2 shows fundus TLR within the posterior pole more prominent temporal to the macula (A). IR image (B) demonstrates an enhanced reflectivity within the area of the TLR. AF image (C) shows speckled regions of enhanced AF around the fovea and a parafoveal ring of AF.

Fig.5 Microperimetry testing results of from each eye of case 2 shows isolated patchy areas of subnormal retinal thresholds within the posterior pole. The right eye is on the right and left eye on the left.

Fig.6 SD-OCT scans of the right eye of case 3 show normal retinal micro-structure and thickness and an increased reflectivity from the RPE-photoreceptor layer complex (A&C). Infrared image (B) shows an enhanced reflectivity within the area of the TLR.

Figure 2
Click here to download high resolution image

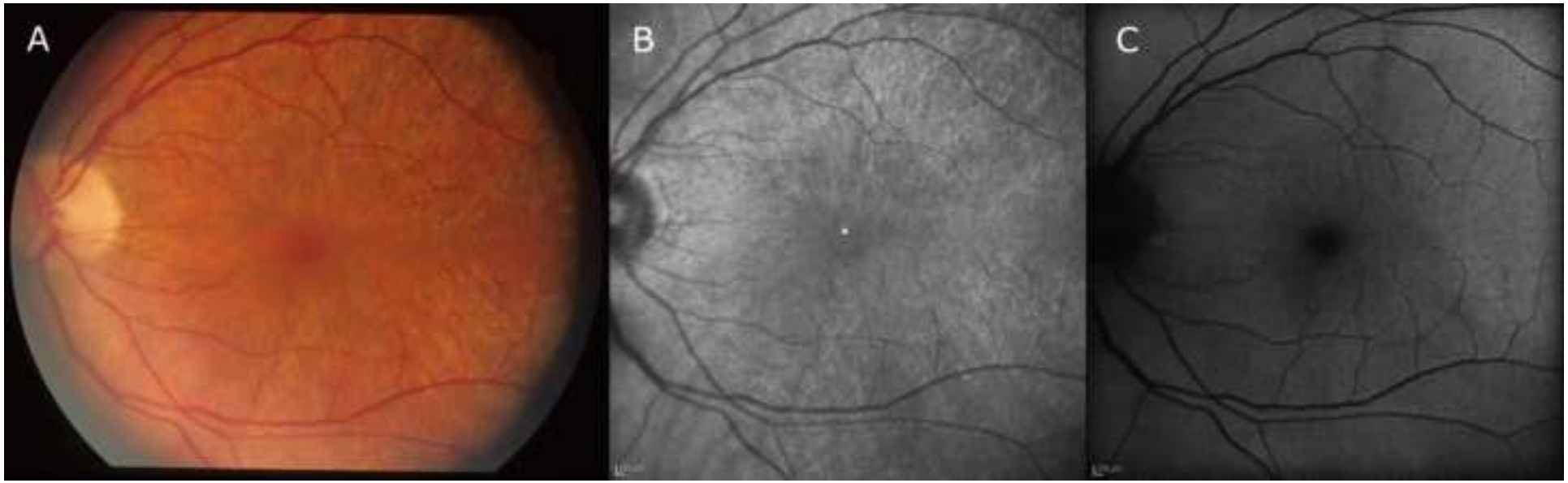

Figure 3

Click here to download high resolution image

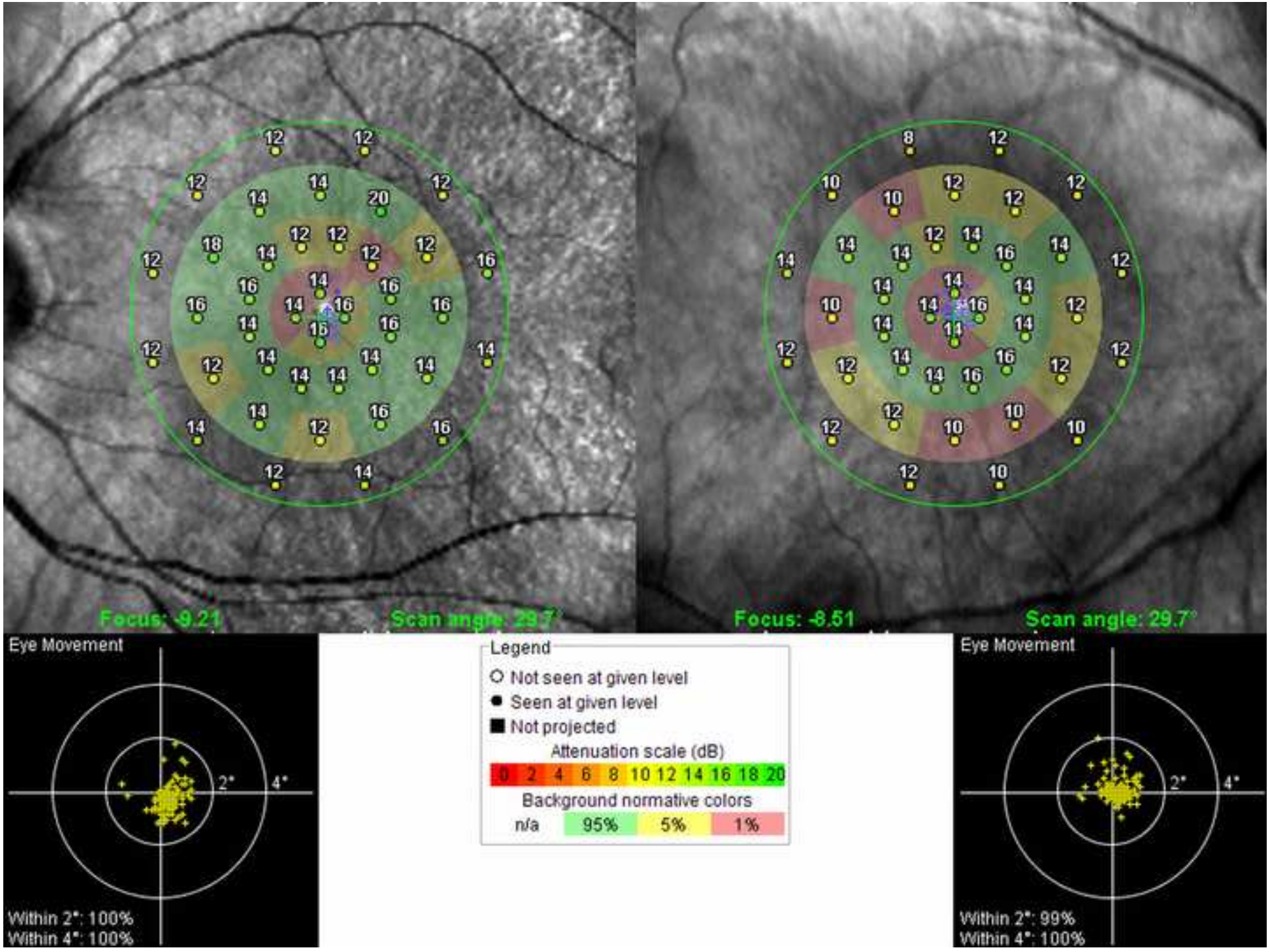

Figure 4
Click here to download high resolution image

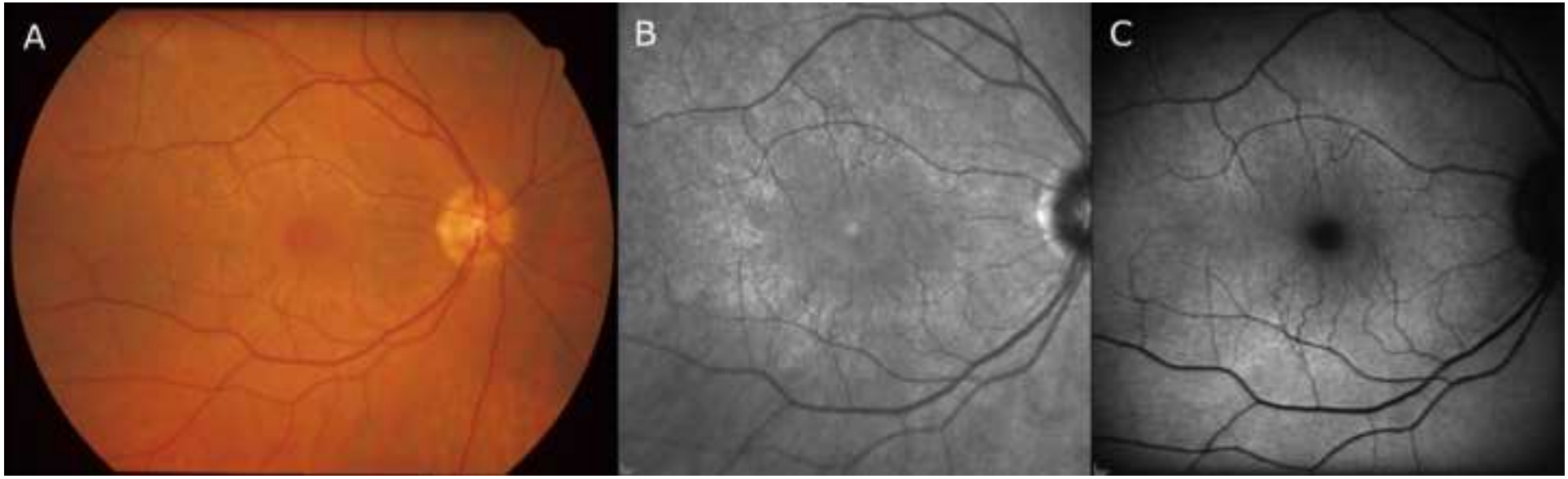

Figure 5

Click here to download high resolution image

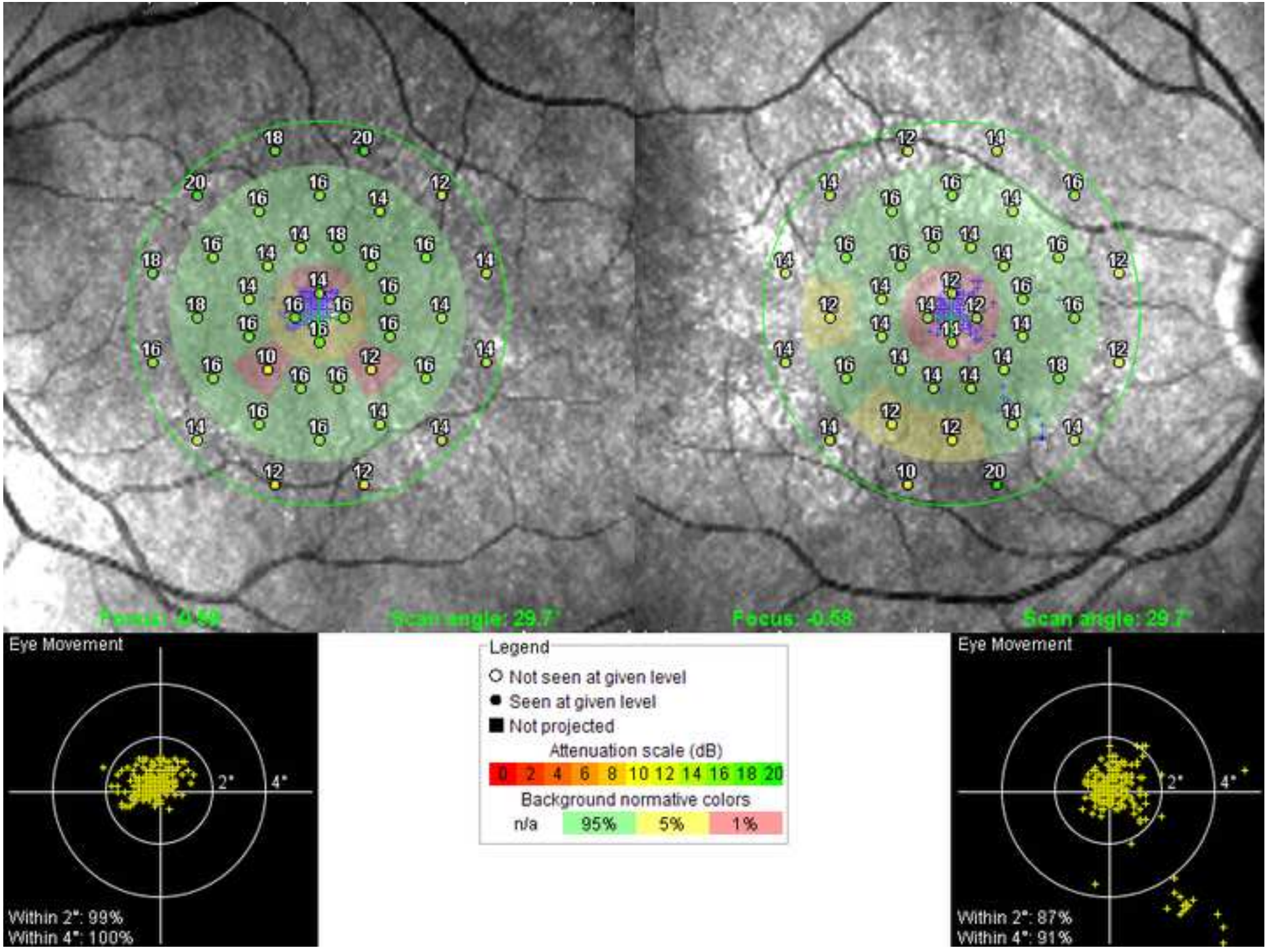

Figure 6

Click here to download high resolution image

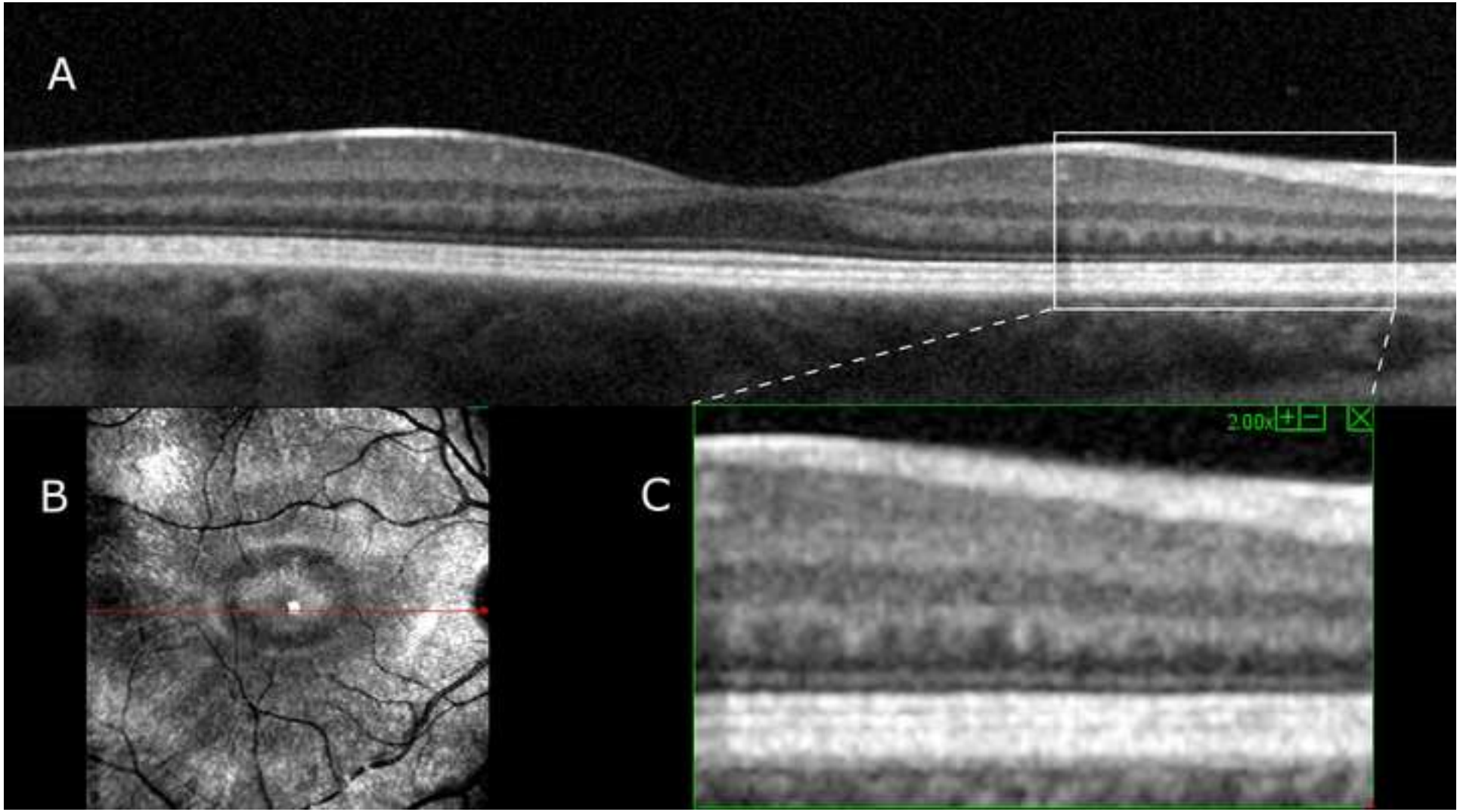

Figure 1

Click here to download high resolution image

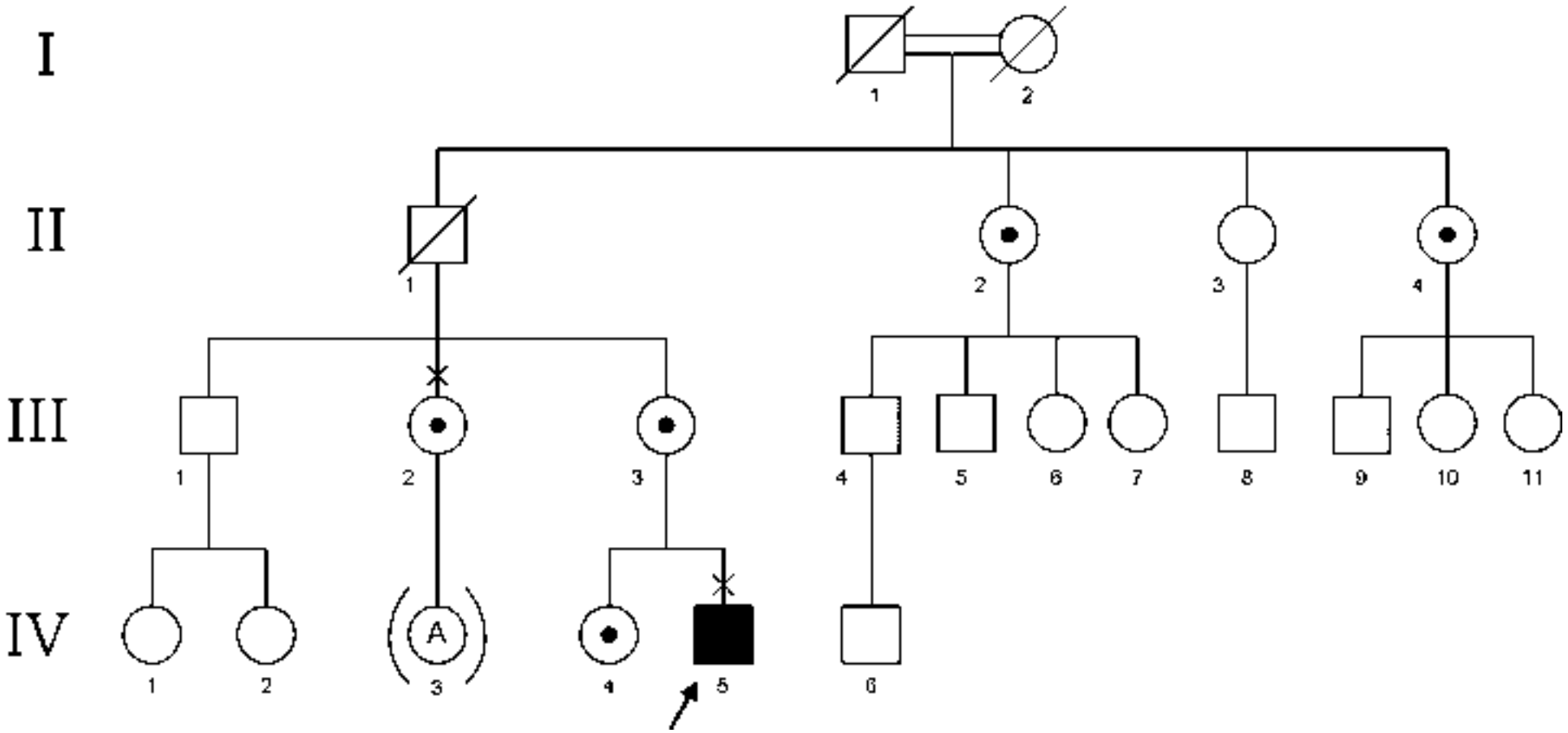

Author Responsibility, Financial Disclosure, and Copyright Transfer Form
Click here to download high resolution image

WORK(S) COVERED UNDER THIS AGREEMENT: This agreement includes all submitted written material as well as any supplementary digital material including but not limited to audio, video, and other data files whose formats may vary.

H. Genad — Mohamed A. Genad — 1/14/2010
Signature — Printed Name — Date
X Author's Own Work ☐ Work for Hire ☐ Government ☐ Financial Disclosure Attached

Gerard Fishman — Gerard Fishman — 1/14/2010
Signature — Printed Name — Date
X Author's Own Work ☐ Work for Hire ☐ Government ☐ Financial Disclosure Attached

Martin Lindeman — MARTIN LINDEMAN — 1/14/2010
Signature — Printed Name — Date
X Author's Own Work ☐ Work for Hire ☐ Government ☐ Financial Disclosure Attached

Signature — Printed Name — Date
☐ Author's Own Work ☐ Work for Hire ☐ Government ☐ Financial Disclosure Attached